

The Reduction of Nitric Oxide by Ammonia over Polycrystalline Platinum Model Catalysts in the Presence of Oxygen

T. KATONA,*†‡ L. GUCZI,*§ AND G. A. SOMORJAI*†

*Center for Advanced Materials, Materials and Chemical Sciences Division, Lawrence Berkeley Laboratory, 1 Cyclotron Road, Berkeley, California 94720; †Department of Chemistry, University of California, Berkeley, California 94720; ‡Department of Organic Chemistry, Jozsef A. University, Dom ter 8, Szeged, H 6720 Hungary; and §Institute of Isotopes, Hungarian Academy of Sciences, P.O. Box 77, Budapest, H 1525 Hungary

Received July 26, 1991; revised January 20, 1992

The reaction system of nitric oxide, ammonia, and oxygen was studied using batch-mode measurements in partial pressure ranges of 65–1000 Pa (0.5–7.6 Torr) on polycrystalline Pt foils over the temperature range 423–598 K. Under these conditions the oxidation of nitric oxide was not detectable. The ammonia oxidation reaction, using dioxygen, occurred in the temperature range 423–493 K, producing nitrogen and water as the only products. The activation energy of the nitrogen formation was found to be 86 kJ/mol. Above this temperature range, flow-mode measurements showed the formation of both nitrous oxide and nitric oxide. The reaction rate between ammonia and oxygen was greatly decreased (about a factor of 10) by nitric oxide, while the reaction rate between nitric oxide and ammonia was accelerated (about 10-fold) due to the presence of oxygen. Nitric oxide reduction by ammonia in the presence of oxygen occurred in the temperature range 423–598 K. The products of the reaction were nitrogen, oxygen, nitrous oxide, and water. The Arrhenius plot of the reaction showed a break near 523 K. Below this temperature the activation energy of the reaction was 13 kJ/mol, and in the higher-temperature range it was 62 kJ/mol. At 473 K, the N_2/N_2O ratio was about 0.6 and O_2 formation was also monitored. At 573 K, the N_2/N_2O ratio was approximately 2 and oxygen was consumed in the course of the reaction as well. © 1992

Academic Press, Inc.

INTRODUCTION

The reduction of nitric oxide to nitrogen is of considerable significance in environmental chemistry. The process must be carried out in the presence of excess oxygen, since in most cases the exhaust gases, which are produced during combustion, contain some unreacted oxygen. The reduction of NO with NH_3 in the presence of O_2 can be carried out over oxide catalysts (VO_x - TiO_x for example), and this catalytic process has been studied in detail (1–3).

The purpose of this paper is to explore the activity of platinum as a catalyst for the reduction of nitric oxide by ammonia in the presence of excess oxygen. Several reactions can occur simultaneously, which could influence the selective catalytic reduction of NO. Accordingly, we have studied:

- (a) NO oxidation;
- (b) NH_3 oxidation;
- (c) the reduction of NO by NH_3 in the presence of O_2 ;
- (d) the decomposition of NO on Pt;
- (e) the decomposition of NH_3 on Pt;
- (f) the reduction of NO by NH_3 in the absence of O_2 .

Here, we focus on reactions (a), (b), and (c). We report on the Pt-catalyzed reactions (d), (e), and (f) in the absence of oxygen in a previous paper (4).

METHODS

Apparatus

A platinum polycrystalline foil with surface area of approximately 2 cm^2 was used as a model catalyst in an ultrahigh-vacuum (UHV)–high-pressure cell that allowed sur-

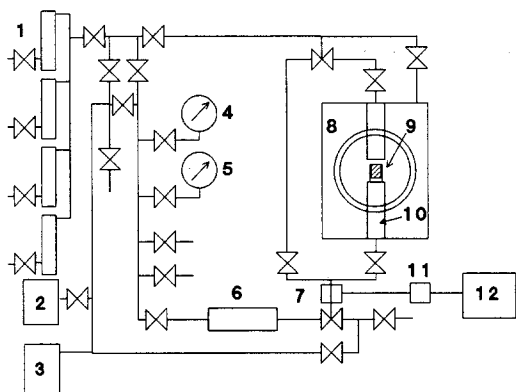


FIG. 1. Schematic diagram of the UHV-high-pressure system with the reaction loop and gas manifold used. (1) Flow meters via reactant gas mixtures were introduced; (2) sorption pump; (3) mechanical pump; (4) high-pressure gauge (10–760 Torr); (5) low-pressure gauge (0.1–20 Torr); (6) Teflon-lined circulation pump; (7) six-way sampling valve; (8) UHV chamber; (9) platinum foil mounted on the manipulator rods; (10) high-pressure cell piston; (11) photoionization detector; (12) gas chromatograph.

face characterization by Auger electron spectroscopy (AES) and permitted us to carry out high-pressure (atmospheric) studies as well. A more complete description of the experimental apparatus is given in Ref. (4). A schematic diagram of the system is shown in Fig. 1. The main vacuum chamber was pumped with a diffusion pump, and $\approx 6 \times 10^{-8}$ Pa (5×10^{-10} Torr) background pressure was achieved after a 24-h bakeout at 473 K. The manipulator, which allowed rotational movement, consisted of two copper rods that held the sample. The Pt foil was spot-welded to gold wires and was heated resistively to the desired temperature using a precision temperature controller. The copper rods were cooled by internal air flow.

Gases

For the reaction, 1% NO in helium, 1% NH₃ in helium, 1% O₂ in helium, and 1% Ar in helium (Matheson certified standards) were used without further purification. The partial pressures of the reactants varied from 70 to 1000 Pa (0.5–7.6 Torr) and the

total pressure was set to 103 kPa (760 Torr), using helium as the balance in order to obtain constant gas circulation speed. For the ion sputtering and oxygen treatments of platinum, high-purity Ar and O₂ (Airco) were used, respectively. High-purity NH₃, N₂O, NO, NO₂, N₂, and O₂ gases (Matheson) were used for calibration.

Experimental Procedure

The platinum foil surfaces were cleaned by a combination of Ar ion sputtering (6.6×10^{-3} Pa (5×10^{-5} Torr) Ar, 2 kV, 30 mA, 15 μ A), O₂ treatment (973 K, 1.33×10^{-4} Pa (1×10^{-6} Torr)) and annealing in UHV to remove surface carbon and other contaminants. The cleanliness of the surface was monitored by Auger electron spectroscopy (15-mA emission, 2 kV, 60- μ A incident current with a 3-mm-diameter defocused beam, 5-V p-p modulation, 50 V/min sweep). The Auger spectrum of the cleaned sample is shown in Fig. 2A.

We used mass spectrometric (MS) analysis with selected ion monitoring (SIM) technique as a detector of gas composition in the high-pressure cell. The hydraulic system that was used to close the high-pressure cell

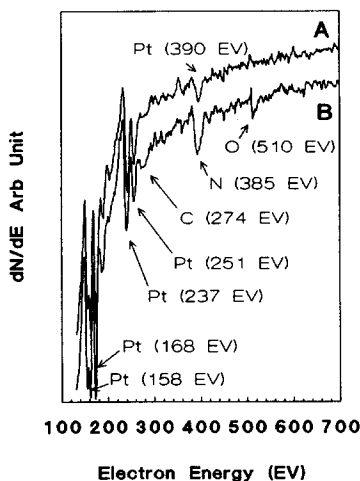


FIG. 2. Auger spectra of platinum foil obtained (A) before the reaction; (B) after the reaction at 473 K in NO + NH₃ + O₂.

was modified to obtain the adjustable and reproducible leak to the chamber. An Ar internal standard was used to calibrate this leak, and intensities were normalized using the Ar MS signal at AMU 40. The calibration of the mass spectrometer was also carried out for each gas we used by introducing different mixtures of pure reactants and He into the high-pressure cell in the same partial pressure ranges as those used for the reactions (4). The background intensities were recorded prior to the reactions and subtracted from the data, keeping in mind the MS sensitivity factors obtained during the calibration (4). The MS was connected to a programmable peak selector (PPS) (UTI 2064). The PPS was on-line connected to an IBM compatible PC via serial communication adapter. The sampling cycle, during which the PPS read all the preset intensities and sent them to the PC, was approximately 6 s. This fast sampling rate allowed us to determine initial reaction rates that were determined by curve-fitting the partial pressure vs reaction time functions.

RESULTS

NO + O₂ (a) Reaction

Within the limits of our mass spectrometric analysis, we did not find any oxidation products of the NO in the temperature range 373–673 K, and partial pressure range 65–1000 Pa (0.5–7.6 Torr), with O₂ to NO ratios of 0.1–10. The sensitivity of the mass spectrometric detection system was 1% conversion. According to the results of the analysis, in our batch-reactor system using excess oxygen, less than 1% of the NO was converted to NO₂ in 30 min at 673 K. Our finding is in agreement with previous results described in the literature (5). The oxidation reaction of the NO occurs at markedly higher temperatures (above 1000 K). Thus we can conclude that in our system and under the conditions that we employed NO oxidation did not take place.

NH₃ + O₂ (b) Reaction

The oxidation of ammonia was detected in the temperature range 423–493 K, at partial

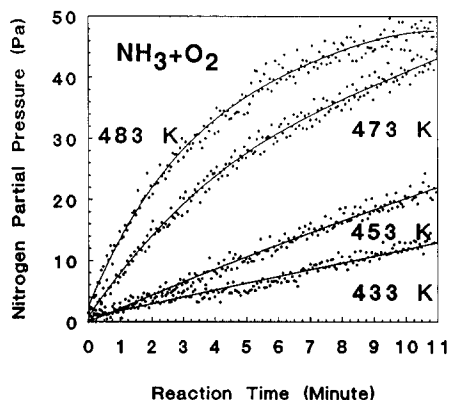
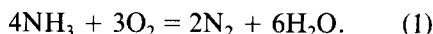


FIG. 3. Nitrogen formation in the NH₃ + O₂ reaction as a function of time at different temperatures using 650:650 Pa (5:5 Torr) NH₃ and O₂ initial partial pressures, respectively.

pressures of NH₃ in 65–650 Pa (0.5–5 Torr) and O₂ partial pressures of 65–1600 Pa (0.5–12 Torr), at NH₃/O₂ ratios from 0.2 to 4. The only products found in this temperature range were N₂ and water, according to the stoichiometric reaction



The temperature dependence of N₂ formation is shown in Fig. 3. The N₂ formation leveled off at about 15% conversion, and gas-phase concentrations reached thermodynamic equilibrium. Above 493 K the reaction became too fast for batch-mode measurements. The Arrhenius plot of the reaction is presented in Fig. 4. The calculated activation energy is 86 kJ/mol.

The initial rate of nitrogen formation showed first-order dependence on the oxygen partial pressure (Figs. 5 and 6), while no NH₃ partial pressure dependence was found in this temperature and pressure range, showing zero-order behavior (Fig. 6).

In order to elucidate the performance of our reactor system and catalyst and to extend the temperature range of our studies, we carried out a few experiments in flow mode as well. Results of the flow-mode experiments are shown in Fig. 7. Above 500 K, nitrous oxide formation, which peaked at

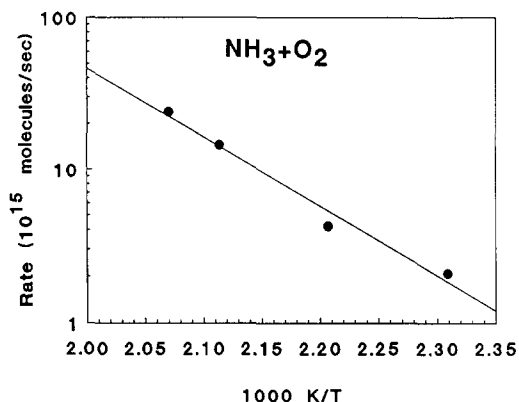


FIG. 4. Arrhenius plot of N_2 formation in $NH_3 + O_2$ reaction using 650:650 Pa (5:5 Torr) of NH_3 and O_2 initial partial pressures.

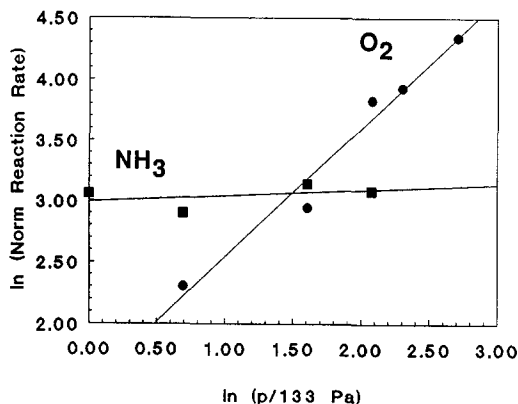


FIG. 6. Nitrogen formation rate as a function of initial O_2 and NH_3 pressures; $\ln(\text{Normalized Rate})$ vs $\ln(p/133 \text{ Pa})$ plot. (●) O_2 ; (■) NH_3 .

about 650 K and became small above 750 K, appeared. Above this temperature, nitric oxide formation was dominant, in agreement with data reported by others.

NO + NH₃ + O₂ (c) Reaction

In the temperature range 423–573 K in the presence of ammonia and oxygen the nitric oxide reacted over the platinum foil. The temperature dependence of NO consumption is shown in Fig. 8. The NO consumption rate was slow compared to the reaction of

the $NH_3 + O_2$ (b) system, which proceeded fast at markedly lower temperatures. However, the nitric oxide consumption was faster than in the $NO + NH_3$ (f) reaction in the absence of oxygen (4). The Arrhenius curve for the reaction showed a break around 523 K (Fig. 9). For the high- and low-temperature regions, activation energies of 62 and 13 kJ/mol were calculated. The product distributions in the two regimes were

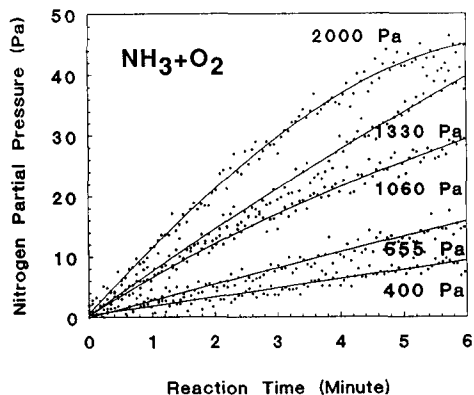


FIG. 5. Nitrogen formation as a function of time at different O_2 initial pressures at 453 K using 650 Pa (5 Torr) NH_3 initial pressures. Initial oxygen pressures are indicated in Pa units.

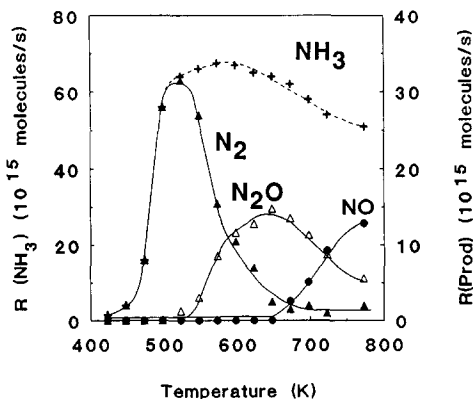


FIG. 7. Temperature dependence of NH_3 consumption rate and the formation rates of products in flow mode using 400:400 Pa (3:3 Torr) NH_3 and O_2 partial pressures. Flow rate: $100 \text{ cm}^3/\text{min}$. The dashed lines shows the value of NH_3 consumption rate (left Y axis). Solid lines show product formation rates (right Y axis). + NH_3 ; (Δ) N_2O ; (●) NO .

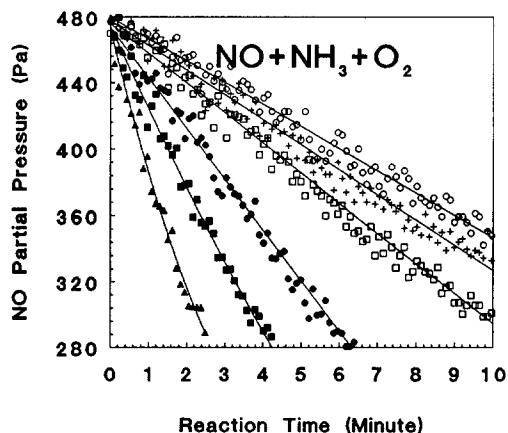


FIG. 8. NO consumption as a function of time in the $\text{NO} + \text{NH}_3 + \text{O}_2$ reaction at different temperatures. Initial partial pressures: 480:400:400 Pa (3.6:3:3 Torr) $\text{NO}:\text{NH}_3:\text{O}_2$. (○) 423 K; (+) 448 K; (□) 473 K; (●) 523 K; (■) 548 K; (▲) 573 K.

different. In the low-temperature region, no O_2 consumption was found. Instead, slow oxygen formation could be monitored (Fig. 10). At 473 K, the $\text{N}_2/\text{N}_2\text{O}$ ratio was approximately 0.6. At 573 K (Fig. 11), oxygen also became a reactant; i.e., it was consumed, and the $\text{N}_2/\text{N}_2\text{O}$ ratio was found to be close to 2. The water formation rate became high compared to that in the low-temperature re-

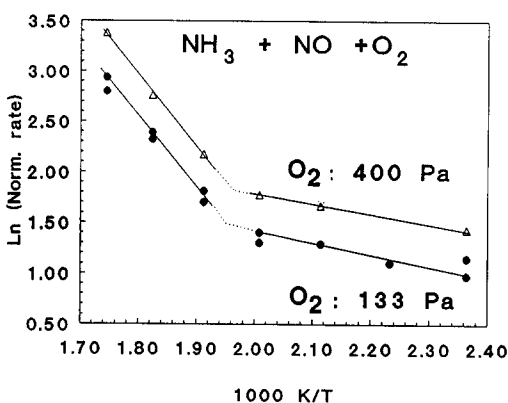


FIG. 9. Arrhenius plots of the rate of NO consumption in the $\text{NH}_3 + \text{NO} + \text{O}_2$ reaction using 133 Pa (1 Torr) and 400 Pa (3 Torr) initial oxygen partial pressures.

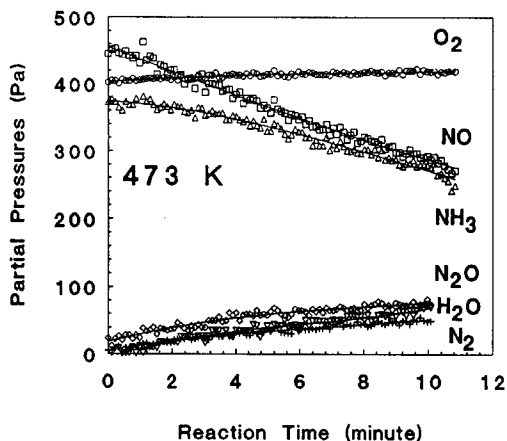


FIG. 10. Partial pressure changes of reactants and products at 473 K as a function of time with 480:400:400 Pa (3.6:3:3 Torr) $\text{NO}:\text{NH}_3:\text{O}_2$ initial partial pressures (□) NO; (Δ) NH_3 ; (○) O_2 ; (+) N_2 ; (◇) N_2O ; (▽) H_2O .

gion. Similar to that for the $\text{NO} + \text{O}_2$ reaction system, we attempted to observe possible NO_2 formation. Within the limits of our experimental detection methods, we did not find evidence for nitrogen dioxide formation in the temperature and partial pressure range we used.

Reaction order studies for NO showed zero-order behavior in the low-temperature region and first-order behavior in the high-

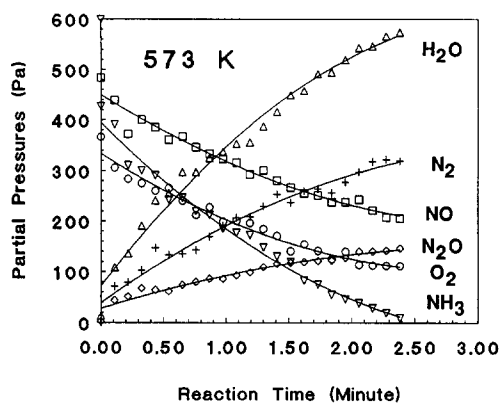


FIG. 11. Partial pressure changes of reactants and products at 573 K as a function of time with 480:400:400 Pa (3.6:3:3 Torr) $\text{NO}:\text{NH}_3:\text{O}_2$ initial partial pressures. (□) NO; (Δ) NH_3 ; (○) O_2 ; (+) N_2 ; (◇) N_2O ; (▽) H_2O .

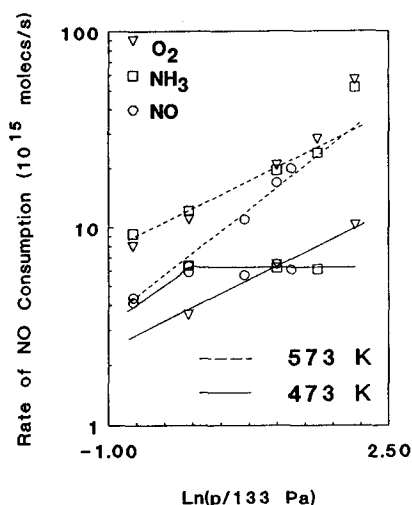


FIG. 12. Results of reaction order studies in the $\text{NO} + \text{NH}_3 + \text{O}_2$ system. Dashed lines, 573 K; solid lines, 473 K. (∇) O_2 ; (\square) NH_3 ; (\circ) NO .

temperature region. The reaction order in NH_3 was zero in the low-temperature regime and became half order at high temperatures. The rate of nitric oxide consumption was half order with respect to oxygen partial pressure in both temperature ranges (Fig. 12).

We did not find oscillations in the $\text{NO} + \text{NH}_3 + \text{O}_2$ (c) reaction system at any temperatures (423–593 K) or partial pressures (65–650 Pa (0.5–5 Torr)), in contrast with the behavior of the $\text{NO} + \text{NH}_3$ (f) reaction system (4) in the absence of oxygen in the temperature range 573–613 K and partial pressures of 65–650 Pa (0.5–5 Torr).

The slow oxygen formation rate in the low-temperature region indicated that nitric oxide or nitrous oxide decomposition did occur on the platinum. We carried out experiments with $^{18}\text{O}_2$ -labeled oxygen in order to explore its role in this temperature region. These experiments showed that no mixed $^{18}\text{O}^{16}\text{O}$ molecules appeared among the products. This indicates that the oxygen formation can be attributed solely to the decomposition of NO or N_2O molecules and no exchange occurs between chemisorbed and gas-phase $^{18}\text{O}_2$ molecules.

Isotopic exchange occurred above 673 K over our Pt foil using 400–400 Pa of $^{16}\text{O}_2$ and $^{18}\text{O}_2$, respectively. This finding is in good agreement with thermal desorption spectroscopic data of O_2 on platinum (Fig. 13). The adsorption was carried out at 120 K, the physisorbed oxygen desorbed below 273 K, and the desorption of dissociated chemisorbed oxygen started above 673 K.

DISCUSSION

$\text{NH}_3 + \text{O}_2$ (b) Reaction

The ammonia oxidation is carried out industrially on Pt–Rh gauze catalysts using high-velocity mixtures of NH_3 and air in the temperature range 1000–1300 K (6). Under those conditions NH_3 can be converted almost exclusively to nitric oxide. The reaction in the high-temperature regime was studied in some detail by others (7, 8); however, it is outside the scope of our present study.

In our experiments, in the temperature range 423–493 K, ammonia reacted with oxygen giving exclusively nitrogen and water as products. Under these conditions, neither nitric oxide nor nitrous oxide formation was found. Our finding is in good agreement with others who investigated the same low-temperature region. For example, Gland and Korchak (9) using stepped platinum single-crystal surface in UHV found that

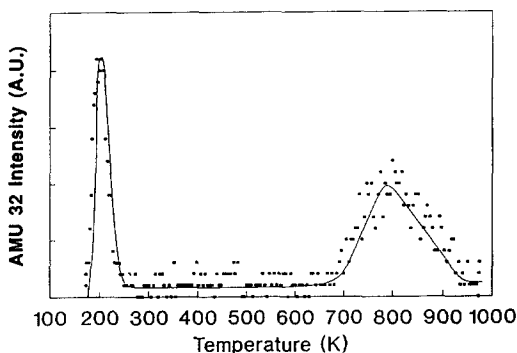


FIG. 13. Temperature-programmed desorption of O_2 from the platinum foil. Exposure: 1 L at 120 K; heating rate 10 K/s.

nitrogen formation was dominant in the 423–673 K region. They also obtained first-order kinetics with respect to oxygen, just as we did. In their experiments the NO formation rate became dominant above 673 K, which is beyond the temperature range (423–493 K) we investigated in batch mode.

Our flow-mode experiments indicated that our platinum foil catalyst performed the well-known ammonia oxidation reaction (Fig. 7). Above 673 K the nitric oxide became the dominant product, in agreement with Ref. (9). The dashed line in Fig. 7 shows the rate of ammonia consumption. Note that at the low-temperature portion of the curve (423–473 K), NH_3 is converted exclusively to N_2 . The maximum in the NH_3 consumption rate of 600 K indicates that the NH_3 coverage is decreased above these temperatures, accounting for the drop in the reaction probability. The same effect was reported by Pignet and Schmidt (11) using Pt wires at various NH_3 and O_2 pressures.

However, in our flow-mode experiments we found N_2O formation, which peaked at about 650 K. This is in agreement with results obtained by Ostermaier *et al.* (10) in the same temperature region using supported platinum catalyst. On the other hand, Pignet and Schmidt (11), using platinum wires in the temperature range 473–1200 K and partial pressures of 13–133 Pa (0.1–1 Torr), reported the lack of N_2O formation even in the low-temperature regime; their only products were NO and N_2 . They explained the found product distribution with an extremely fast reaction that occurred between the ammonia and oxygen, giving NO as product, even in the low-temperature range. This NO, which was relatively strongly bound to the surface, reacted further without desorbing, giving nitrogen, the other product of the reaction; i.e., the N_2 formation was due to the reaction between chemisorbed NH_3 and NO. As the temperature increased, more NO could escape from the surface causing higher NO/ N_2 ratio.

In our case, in this temperature region (423–493 K), only N_2 formation was found,

and adding NO to the reaction mixture strongly inhibited the rate of nitrogen formation and caused considerable N_2O formation. Unlike Schmidt's platinum wires, the performance of our catalyst did not show dependence on the catalyst history; we obtained the same specific reaction rates and product distributions on many foils after cleaning our samples by ion sputtering and oxygen annealing in UHV. From this point of view, our platinum surface was similar to those prepared by Gland and Korchak (9) using UHV techniques. It appears that the method of preparation rather than the employed pressure range of reactants determines the catalytic behavior of Pt in this reaction. In addition, the nitrogen formation rate, as a consequence of the $\text{NH}_3 + \text{O}_2$ (b) reaction at these relatively low temperatures, was an order of magnitude higher than in the case of $\text{NO} + \text{NH}_3$ (f) reaction; thus we believe that the primary product of $\text{NH}_3 + \text{O}_2$ reaction is N_2 and not NO at these low temperatures, over polycrystalline platinum foils.

$\text{NH}_3 + \text{NO} + \text{O}_2$ (c) Reaction

(1) *Low-temperature regime (423–523 K).* Our studies showed that NO reduction occurred in the presence of oxygen in the temperature range 423–598 K at partial pressures of 65–650 Pa (0.5–5 Torr) of NO and NH_3 and up to 1000 Pa (7.6 Torr) of oxygen. The Arrhenius curve of the NO consumption showed a break at 523 K. At 473 K, using 480-Pa NO and 400–400 Pa of NH_3 and O_2 , the $\text{N}_2/\text{N}_2\text{O}$ ratio was found close to 0.6. At this temperature the reaction order for both NO and NH_3 was zero. The NO consumption rate showed half-order kinetics with respect to oxygen partial pressure. This suggests that dissociatively adsorbed oxygen is involved in the rate-limiting step in both the low-temperature and the high-temperature regions as well. However, in the low-temperature range, oxygen was not consumed, but a small amount was formed. The primary source of the oxygen is the

nitric oxide molecule, and the O_2 formation rate is $12 \pm 3\%$ of the NO consumption rate.

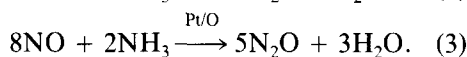
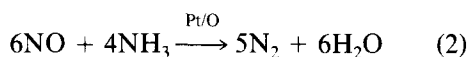
Oxygen is believed to adsorb on platinum dissociatively, and we did find half-order oxygen partial pressure dependence. This means that dissociatively adsorbed oxygen is involved in the formation of a catalytically active site. The use of $^{18}O_2$ showed that neither oxygen consumption nor oxygen scrambling occurred during the reaction in the low-temperature range. This is difficult to understand and more work is needed to verify the mechanisms responsible for these findings. It is possible that a static chemisorbed oxygen layer or islands are formed on the surface with a coverage that is oxygen pressure dependent, and the reaction proceeds either on that layer or at its interface with the metal. This surface compound remains intact during the reaction and no detectable exchange with the gas-phase O_2 or NO occurs.

The use of $^{16}O_2$ and $^{18}O_2$ showed that scrambling starts above 673 K. This is the temperature at which the desorption of chemisorbed oxygen starts, according to the TPD data (Fig. 13). It indicates that the chemisorbed layer can be formed at lower temperatures and may remain stable. It has been shown that the formation of platinum oxide is thermodynamically favorable in the temperature and pressure range we employed (12).

The oxygen formation in the low-temperature range (Fig. 10) can be the consequence of several parallel reactions, such as the decomposition of nitric oxide ($2NO = N_2 + O_2$), the decomposition of nitrous oxide ($2N_2O = 2N_2 + O_2$), and the formation of nitrous oxide ($4NO = 2N_2O + O_2$) in the presence of ammonia and oxygen.

(2) *High-temperature regime* (523–593 K). In the high-temperature range the N_2/N_2O ratio was about 2, and oxygen consumption was detected. At 573 K, the NO consumption rate was first order with respect to NO partial pressure, half order with respect to NH_3 partial pressure, and half order for the oxygen partial pressure as well.

In the high-temperature region NH_3 consumption rate was enhanced, and a considerable amount of water was formed. This resembles the behavior of the $NH_3 + O_2$ reaction (Eq. (1)); however, at this temperature, the reaction between the ammonia and oxygen would be very fast, giving nitrogen and nitrous oxide as products. On the other hand, NO consumption is also remarkably high and is catalyzed by the presence of oxygen on the platinum surface. Thus among the possible parallel reactions are the $NH_3 + O_2$ (Eq. (1)), and the $NO + NH_3$ (Eqs. (2) and (3)) leading to either N_2 or N_2O :



(3) *Work by others*. It appears that oxygen plays an essential role in the reaction as indicated already. Michailova (13) found that oxygen pretreatment deactivated the catalyst (platinum wire) she used. In contrast, Gland and Korchak (9) did not find an oxygen effect on the reaction rate in UHV. Pignet and Schmidt (11), using steady-state measurements in the pressure range 10–266 Pa, reported a higher reaction rate in the presence of oxygen on platinum wires. This effect was attributed to the removal of surface contaminations by oxygen at lower temperatures.

Tsai *et al.* (14, 15) also reported higher NO reduction rate using supported Pt catalysts in the temperature range 373–423 K at atmospheric total pressures using partial pressures in the range of our experiments. The higher reaction rate was explained as follows: The oxygen inhibits the oxidation of platinum by NO. Using polycrystalline platinum foil together with the supported platinum catalyst in the reactor bed, the foils were then put into UHV, exposing them to air. AES depth profile measurements showed that when no oxygen was present in the reaction mixture, more oxygen was found in the submonolayer.

However, it was shown that in UHV, NO

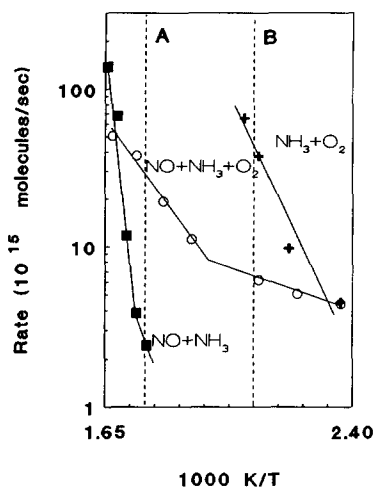


FIG. 14. Comparison of Arrhenius plots of reaction systems (b), (c), and (f). (■) $\text{NO} + \text{NH}_3$ (f); (○) $\text{NO} + \text{NH}_3 + \text{O}_2$ (c); (+) $\text{NH}_3 + \text{O}_2$ (b).

can oxidize platinum only above 773 K (16). Furthermore, we did not find evidence for Tsai's results; in our experiments our platinum foils did not show oxygen Auger peak after the $\text{NO} + \text{NH}_3$ (f) reaction, in the absence of oxygen (4).

Markvart and Pour (17) also reported enhanced reaction rate when oxygen was present in the reaction mixture. His proposed explanation was that oxygen accelerated the reaction by enhancing the dissociation of the ammonia on the surface, shifting its equilibrium toward more reactive species.

The effect of oxygen was found to correlate with the crystallite size on supported platinum catalyst as well (18). When oxygen was present the reaction became structure sensitive.

There seems to be agreement in the literature about the effect of the oxygen on the product distribution. When oxygen is present, the $\text{N}_2/\text{N}_2\text{O}$ ratio is decreased considerably.

(4) *Comparison of $\text{NO} + \text{NH}_3$ reaction in the absence and presence of oxygen.* In Fig. 14, comparison of the Arrhenius curves of reactions (b), (c), and (f) is shown. The ammonia oxidation reaction (b) is plotted using

NH_3 consumption rates, and the $\text{NO} + \text{NH}_3$ (f) and $\text{NO} + \text{NH}_3 + \text{O}_2$ (c) reactions are plotted using NO consumption rates as a function of temperatures. At 573 K (dashed line A) the NO consumption is about one order of magnitude higher when oxygen is present (c) than when oxygen is absent (f). If the trend of the NH_3 consumption in the $\text{NH}_3 + \text{O}_2$ reaction (b) continued, it would be approximately one and a half orders of magnitude higher than in the case when NO is also present in the reaction mixture (c). The same effect can be seen along dotted line B (473 K). When NO is added to the $\text{NH}_3 + \text{O}_2$ system (b), the reaction rate is decreased (c), and the addition of oxygen increases the rate of the reaction between the $\text{NO} + \text{NH}_3$ (f). Thus, we can conclude that the NO inhibits the reaction between the ammonia and oxygen, and oxygen catalyzes or promotes the reaction between ammonia and nitric oxide. These effects can be easily demonstrated using reactant compositions far from the stoichiometric mixture. When nitric oxide is in large excess in the $\text{NO} + \text{NH}_3 + \text{O}_2$ reaction mixture, the NO consumption rate stops when all the ammonia is consumed. When NH_3 is in large excess, N_2 formation rate jumps after NO is consumed. At higher temperatures, when oxygen is consumed (using less oxygen than required by the reaction stoichiometry), the NO consumption rate drops to that of the $\text{NO} + \text{NH}_3$ (f) reaction rate.

In the absence of oxygen, the Arrhenius plot of reaction (f) also shows a break (4). In the low- and high-temperature regions, $\text{N}_2/\text{N}_2\text{O}$ ratios of 1 and 10–15 were found, respectively. These data show similar trends to our observations for the $\text{NH}_3 + \text{NO} + \text{O}_2$ system (c), where the corresponding values were 0.6 and 2, respectively.

Apparently, the break in the Arrhenius curve, the different activation energies, and the product distributions correspond to different reaction patterns in the low-temperature and high-temperature regions. Because of the complexity of this reaction system the

divergence of the literature data is understandable.

In the temperature range of the break on the Arrhenius curve in the absence of oxygen, the transition between the two regions was accompanied by rate oscillations (4). When oxygen was present, no oscillations occurred under any conditions. In fact, the oscillations were very sensitive to the presence of oxygen. When less than 0.1% of oxygen was added, oscillations have stopped.

SUMMARY

The reaction system of NH_3 and NO was studied over polycrystalline Pt foils in the temperature range 423–598 K at atmospheric total pressure using reactant partial pressures in the range 65–1000 Pa (0.5–7.6 Torr). In this pressure and temperature range, no NO oxidation occurred while the reaction between the NH_3 and O_2 proceeded rapidly. The only products we observed in this reaction in the temperature range 423–493 K were N_2 and H_2O . The Arrhenius plot of the $\text{NO} + \text{NH}_3 + \text{O}_2$ reaction system showed a break near 523 K. Using batch-mode measurements, two well-distinguishable reaction patterns can be identified. The rate of NO reduction at low temperatures shows zeroth reaction order with respect of NO and NH_3 , while in the high-temperature range first and half orders with respect to NO and NH_3 were found, respectively. The reaction order for oxygen was found to be 0.5 over the whole temperature range that we explored. The activation energies were 13 and 62 kJ/mol for the low-temperature range and for the high-temperature range, respectively. In the low-temperature regime no oxygen consuming process was detectable; i.e., no ammonia burning took place. As compared to the results obtained in the absence of

oxygen (4) we can conclude that nitric oxide inhibits the reaction between ammonia and oxygen, while oxygen accelerates the reaction between nitric oxide and ammonia in both temperature ranges.

ACKNOWLEDGMENTS

This work was supported by the Director, Office of Energy Research, Office of Basic Energy Sciences, Materials Science Division, U.S. Department of Energy, under Contract No. DE-AC03-76SF0098. The authors thank Johnson Matthey Co. for their financial support.

REFERENCES

1. Keith, C. D., and Kenah, M., US Pat., 3,328,115 (1967).
2. Griffing, M. E., Lamb, F. W., and Stephens, R. E., US Pat., 3,449,063 (1969).
3. Odriozola, J. A., Heinemann, H., Garcia de la Banda, J. F. Pereira, P., and Somorjai, G. A., *J. Catal.* **119**, 71 (1989).
4. Katona, T., Guzzi, L., and Somorjai, G. A., *J. Catal.* **132**, 440 (1991).
5. Papapolymeru, G. A., and Schmidt, L. D., *Langmuir* **1**, 488 (1985).
6. Contour, J. P., Mouvier, G., Hoogewys, M., and Leclere, C., *J. Catal.* **48**, 217 (1977).
7. Asscher, M., Guthrie, M. L., Lin, I. H., and Somorjai, G. A., *J. Phys. Chem.* **88**(15), 3234 (1984).
8. Hsu, D. S. Y., and Lin, M. C., *Appl. Surf. Sci.* **28**, 451 (1987).
9. Gland, J. L., and Korchak, V. N., *J. Catal.* **53**, 9 (1978).
10. Ostermaier, J. J., Katzer, J. R., and Manogue, W. H., *J. Catal.* **33**, 457 (1974).
11. Pignet, T., and Schmidt, L. D., *Chem. Eng. Sci.* **29**, 1123 (1974).
12. Peuckert, M., *J. Phys. Chem.* **89**, 2482 (1985).
13. Michailova, E. A., *Acta Physicochim. URSS* **10**, 653, (1939).
14. Tsai, J., Agraval, P. K., Sullivan, D. R., Katzer, J. R., and Manogue, W. H., *J. Catal.* **61**, 192 (1980).
15. Tsai, J., Agraval, P. K., Sullivan, D. R., Katzer, J. R., and Manogue, W. H., *J. Catal.* **61**, 204 (1980).
16. Gland, J. L., and Korchak, V. N., *J. Catal.* **55**, 324 (1978).
17. Markvart, M., and Pour, V., *J. Catal.* **7**(3), (1967).
18. Pusateri, R. J., Katzer, J. R., and Manogue, W. H., *AIChE J.* **20**, 219 (1974).